ELSEVIER

Geoderma 70 (1996) 231–252

GEODERMA

Simulation of gravity fingering in porous media using a modified invasion percolation model

R.J. Glass, L. Yarrington

Sandia National Laboratories, Albuquerque NM 87185-1324, USA

Received 1 October 1994; accepted 20 January 1995

Abstract

We introduce a modified invasion percolation (MIP) model for the immiscible displacement of a nonwetting fluid by a wetting fluid within a porous network. The model includes the influence of gravity and is applicable in the quasi-static limit of infinitesimal flow rate where viscous forces are negligible with respect to gravity and capillary forces. The incorporation of gravity alone creates complicated, pore-scale gravity fingers. To properly model wetting fluid invasion where macroscopic gravity fingers form, we incorporate a pore-scale geometric capillary smoothing function we refer to as "facilitation." Facilitation models the physics of wetting fluid invasion of pores by modifying the capillary pressure required to fill a pore based on the number of adjacent necks connecting the pore to the invading wetting fluid. The wetting fluid invasion facilitation process creates compact clusters and macroscopic fronts in horizontal simulations and in combination with gravity, creates macroscopic, gravity fingers that are in qualitative agreement with physical experiments. The MIP model yields much different imbibition front structures than standard invasion percolation. For MIP, capillary fingering, capillary facilitation, and gravity fingering compete to determine the wetted network structure as a function of pore-size distribution.

1. Introduction

Gravity-driven fingering of water in air-filled, water-wettable porous media and fractures has been studied in a number of laboratory experiments since its discovery in the early 1960's (see reviews in papers contained in this special issue of Geoderma). While understanding of the phenomenon has greatly advanced over this period, the effects of a number of complicating factors ubiquitous under field conditions are yet to be fully explored. The influence of uniform and non-uniformly distributed initial moisture content, media heterogeneity, and macropores and fractures were discussed by

Elsevier Science B.V.
SSDI 0016-7061(95)00087-9

Glass and Nicholl (1996). All of these factors have the ability to fundamentally affect the fingering process, its scale of expression, or suppress its occurrence entirely. In addition to these factors, the properties of the media/fluid/fluid system, as influenced by pore shape and pore-size distribution, control gravity fingering.

In this paper, we explore pore-scale controls on gravity finger formation and water swept structure at the quasi-static, low flow limit (i.e., small capillary number). We begin with a description of observed pore-scale finger advancement. This observed behavior is used as a basis to formulate a conceptual model, a modified form of invasion percolation, which incorporates the Haines jump pore-filling mechanism, gravity, and a pore-scale geometric interfacial capillary smoothing function we call adjacent-neck-pore-filling "facilitation". Facilitation accounts for the combined effects of surface tension, pore geometry, and contact angle that must be incorporated to properly model the spontaneous imbibition of a wetting fluid into a non-wetting fluid filled porous media. To demonstrate model behavior, we implement the modified invasion percolation (MIP) for a two-dimensional and quasi-three-dimensional network of two-dimensional pores. We explore a single random pore network hierarchy within which we vary idealized pore geometries (and thus facilitation) and size distributions. The wetted structures and fingers that evolve under horizontal and vertical downward infiltration are found to be dependent on both the pore geometries and the pore-size distribution. This dependence exhibited by MIP is absent in standard invasion percolation models.

2. Formulation of conceptual model

A gravity finger in an initially dry, clean, narrow distribution sand, is composed of a nearly saturated tip that drains a distance behind its leading edge as the finger grows downward (Glass et al., 1989c). Finger tips are essentially short, nearly saturated, hanging water columns which are fed from above under near unit gradient at a rate determined by the relative permeability of the transmission zone connecting the nearly saturated tip to the fluid source. The length of the saturated zone (L_s) of all finger tips is found to be greater than the difference between air-entry value (ψ_{ae}) and the water-entry value (ψ_{we}) of the hysteretic pressure–saturation relation ($\Delta\psi$) (Glass et al., 1989c).

As flow rate increases to the system, finger velocity, finger width, and L_s increase and in the "high flow" limit a stable one-dimensional flow field is forced (Glass et al., 1989a, Glass et al., 1989b). Thus, while gravity fingering is considered to be a highly dynamic process, observations show that raising the total system energy by increasing the system flow rate actually stabilizes the flow field; thereby decreasing complication. It should be noted that the converse is true for viscous-driven fingering (Saffman and Taylor, 1958).

At "low flow," where gravity fingering will dominate the flow field, the system dynamics are primarily confined to the front and back of the nearly saturated finger tip. There, localized Haines jumps occur as the meniscus in an individual pore becomes unstable and moves rapidly to fill or empty the pore at a rate determined by local capillary, viscous, and inertial forces. In addition to the Haines jump mechanism, liquid also moves as films from wet regions to dry. However, film flow in clean, narrow

grain-size distribution sands is quite slow in comparison to the rapid pore filling associated with Haines jumps. The film flow mechanism is responsible for the long-term development of a two-zone moisture content field under steady infiltration as demonstrated by Glass et al. (1989c). In their experiment, fingers moved through the sand system in a matter of minutes, while the growth of the unsaturated film flow region occurred over several days. These observations emphasize the dramatically different time scales for the two separate wetting mechanisms in clean, narrow grain size distribution sands.

Because finger growth is controlled primarily by the Haines jump mechanism, as long as the time scale for finger growth is much shorter than that for film flow along the grain edges, and slow enough for discrete jumps to occur (i.e., negligible viscous forces), a pore-scale model that incorporates only the Haines jump mechanism is appropriate. Here, capillarity and gravity combine to dictate growth by determining which pore is filled next (i.e., has the lowest potential required for filling). For this situation, a form of invasion percolation (IP) should apply.

The IP process, introduced by Wilkinson and Willemsen (1983), models imbibition where the pressure potential within the wetted region does not vary in space. This is a reasonable assumption in the quasi-static limit of infinitesimal flow rate where viscous forces are negligible and the system is dominated by capillary (surface tension) forces. IP occurs as follows:

(1) A pore network of a given connectivity is generated with each pore given a probability of filling.

(2) Certain pores are filled initially to form a boundary wetting surface, usually either an edge of a rectangular network or a disk at the center.

(3) All pores connected to the wetted pore surface are available for filling and the one with the highest assigned probability of filling is found and filled. This modifies the list of pores available for filling; the modified list is then sorted to once again find the pore with the highest assigned probability of filling. This pore is filled, the list modified, and so on.

(4) Pores that become entrapped may or may not be removed from the pores available to be filled depending on the situation of interest. If the defending fluid can be assumed incompressible, then removal is appropriate, while if the fluid is infinitely compressible or dissolvable, then entrapped pores should not be removed.

IP has been shown to conform reasonably well to the invasion by a nonwetting fluid of a porous medium composed of a two-dimensional, horizontal, random pore network; the fluid–fluid interface under such conditions exhibits structure at all scales down to the pore-scale, and has been shown to be fractal (Lenormand and Zarcone, 1985). For wetting fluids invading porous networks as considered here, interfaces are much smoother and macroscopic fronts characteristically form (Lenormand and Zarcone, 1984). To apply IP to our problem, we must, therefore, modify it both to include gravity and to conform to the physics of wetting fluid invasion.

To include gravity forces in proper magnitude with capillary forces, we cast the probability of filling in terms of a pore-filling potential. This approach was first applied by Wilkinson (1984) to study the effect of gravity forces on the mixing region between two vertically stratified immiscible fluids. Here, the pore radius becomes the random

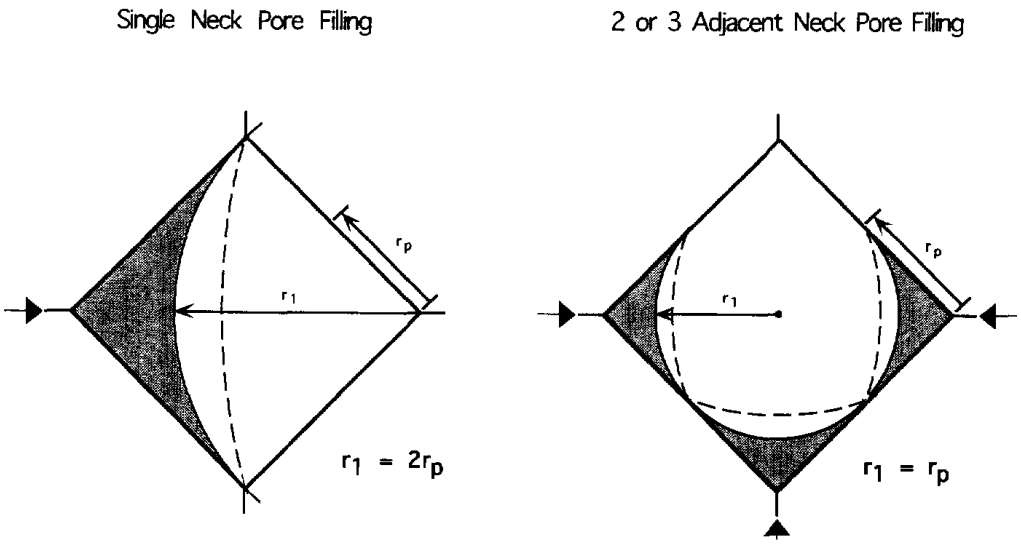

Fig. 1. Simple geometric argument for adjacency dependent, pore-filling radius for an idealized two-dimensional square pore. In the figure on the left the pore is fed (gray denotes water, white air) from the left by one neck. The pore fills by a Haines jump when the pore-filling radius, r_1, reaches two times the pore radius, r_p, given by that of a circle circumscribed by the square. If the pore is filled by either two or three adjacent necks (right figure) then the menisci will touch when r_1 equals r_p yielding a lower pressure potential required to fill the pore. This adjacent-neck–pore-filling facilitation can be determined for a variety of different pore shapes and contact angles. The effect of a non-zero contact angle is illustrated by the dashed line.

variable. Pore-filling potential is calculated as the sum of the pressure potential and gravity potential. Pore-filling pressure potential is given by the Laplace–Young relation between the two principal radii of interfacial curvature (r_1 and r_2), surface tension (σ), the fluid density difference ($\Delta\rho$), gravitational acceleration (g), and the capillary pressure potential difference across the interface (ψ_p):

$$\psi_p = \frac{-\sigma}{\Delta\rho g}\left(\frac{1}{r_1} + \frac{1}{r_2}\right) \tag{1}$$

Gravity potential (ψ_g), is simply given by:

$$\psi_g = -z\cos\gamma \tag{2}$$

where z is the spatial coordinate defined positive downward from the top of the network and γ is the angle between vertical and the plane of the network.

For wetting fluid invasion of a porous media, the principal radii of curvature at the point when the pore will fill depends on local pore geometry, contact angle, and the number of adjacent necks connecting the pore to the filled interface and through which the pore will fill. Neglecting the details of the neck–pore connection, the simple geometric argument for adjacency dependence is shown for an idealized two-dimensional square pore (r_2 becomes infinite) in Fig. 1. Note that the illustration depicts the point beyond which a Haines jump occurs. When filling from a single neck (corner), the pore-filling radius r_1 is equal to the side of the square or twice the pore radius, r_p, given

by the circle circumscribed by the square. If more than one surrounding pore is filled such that two, three, or four adjacent necks are filled, then due to the touching of menisci from each neck, r_1 is reduced to r_p. Of course, if the nonwetting fluid is not infinitely compressible, with four adjacent necks filled, the pore is entrapped and the nonwetting fluid can not be displaced. Thus, when one or more adjacent necks are filled, the curvature required to fill the pore is increased (r_1 decreased). We have coined the term adjacent-neck–pore-filling facilitation or simply "facilitation" for this effect as it lowers the pressure potential at which a pore fills. This argument for simple two-dimensional geometries can be extended in principle to three-dimensional pores of complex geometery.

While the filling of a pore with the wetting fluid is determined by the pore-filling radius and connection to the wetting interface, drainage of a pore is governed by the radii of the necks and the connection of pores through the necks to the air filled interface. Once the total potential within a pore filled with the wetting fluid has decreased below that required to empty one of the necks connecting it to the air filled interface, both neck and pore empty immediately. Thus, assuming that a single neck is not connected to more than two pores, the invasion of a pore by the non-wetting phase is not affected by a facilitation mechanism and standard invasion percolation on the network of necks and pores, independent of adjacency, should apply.

3. Model implementation and numerical simulation

While the modified invasion percolation model (MIP) introduced above is conceptually very simple, implementation requires that the exact geometry of the three-dimensional pore network within a porous medium be known. This, of course, is only now becoming technically possible and for only limited sample sizes (e.g., Adler et al., 1992). As a first step toward understanding the implications of the pore network MIP model for simulating the growth of a gravity finger, we consider here an idealized, regular pore network with idealized pores of specific geometry. As above, we consider necks connecting pores to be much smaller than the pores and to not pin invading menisci, i.e., the detailed geometry of the necks and neck-pore connections is negligible compared to that of the pore for wetting invasion. We further constrain ourselves to two-dimensional pore geometry (r_2 infinite) on two-dimensional and quasi-three-dimensional networks so that facilitation may be calculated exactly. Finally, we implement only the wetting process within a simulation; inclusion of the simultaneous wetting and drainage of pores within a simulation adds significant complication that is not required to consider the pore-scale controls on gravity finger formation and water swept network structure.

The two-dimensional network is abstracted as a regular array of two-dimensional pores connected to each other by necks. Since this study is only concerned with wetting fluid invasion, necks connected to a pore always fill when the pore fills. Pores are centered on a regular square lattice, 256 pores wide by 512 pores long with a macroscopic dimension 2.55 cm wide by 5.11 cm long. Pore connectivity is constant for the entire network with a coordination of 4 or 8. In the network configuration for a

Table 1
Formulas for pore filling radius

Square:	
no adjacent necks:	$r_l = \frac{2r_p \tan(45+\theta)}{\cos\theta + \sin\theta}$
2, 3, or 4 [a] adjacent necks:	$r_l = \frac{r_p \tan(45+\theta)}{\cos\theta + \sin\theta}$
Octagon:	
no adjacent necks:	$r_l = \frac{2r_p \tan(67.5+\theta)}{\tan(67.5)\cos\theta + \sin\theta}$
2 adjacent necks:	$r_l = \frac{2r_p(1+1/\sqrt{2})\tan(45+\theta)}{\tan(67.5)[\cos\theta + \sin\theta]}$
3 adjacent necks:	$r_l = \frac{2r_p[1+\tan(67.5)]\tan(22.5+\theta)\tan(22.5)}{\tan(67.5)[\tan(22.5)\cos\theta + \sin\theta]}$
4, 5, 6, 7, or 8 [a] adjacent necks:	$r_l = \frac{r_p \tan(67.5+\theta)}{\tan(67.5)\cos\theta + \sin\theta}$

[a] Only applicable to infinitely compressible fluids.

coordination of 8, diagonal connections are made that do not communicate with each other at the crossing point. This configuration mimics a three-dimensional network with every other pore (both vertical and horizontal) on each of two parallel planes (Wilkinson and Willemsen, 1983).

We explore two idealized two-dimensional pore shapes where facilitation can be calculated exactly: squares (coordination 4) and octagons (coordination 8). The pore radius (r_p) denotes the radius of a circle that would be circumscribed by each, respectively. Formulas based on two-dimensional pore geometry and contact angle (θ) for the calculation of the pore-filling radius r_l from r_p considering facilitation are given in Table 1. Note that contact angles much less than 90 degrees result in non-wetting pores (e.g., above 45 degrees for the square pores and above 22.5 degrees for the octagon pores). For simplicity, contact angle is taken to be zero.

Because reasonable estimates of minimum and maximum pore sizes are available as well as mean and variance, the maximum entropy principle suggests the use of a Beta distribution for describing the r_p distribution (Harr, 1987). Therefore, we choose r_p from the Beta probability distribution defined over the range $[r_{min}, r_{max}]$ by:

$$f(r_p) = C(r_p - r_{min})^{\alpha}(r_p - r_{max})^{\beta} \tag{3}$$

where $\alpha > -1$ and $\beta > -1$. If α and β are integers, the normalizing constant (C) is given by:

$$C = \frac{(\alpha+\beta+1)!}{\alpha!\beta!(r_{max} - r_{min})^{\alpha+\beta+1}} \tag{4}$$

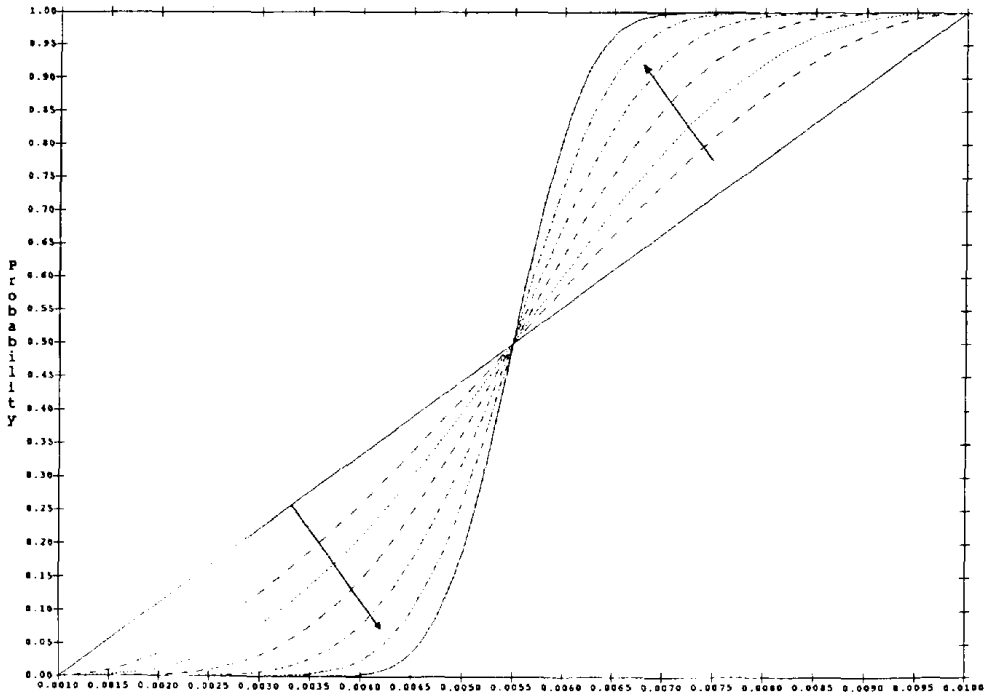

Fig. 2. Plot of the cumulative Beta probability distributions used in this study to represent pore sizes. Only symmetrical distributions are explored; where $\alpha = \beta = (0, 1, 2, 4, 8, 16, 32)$ in the interval 0.001 to 0.01 cm. Increasing $\alpha = \beta$ is denoted by the arrows.

Here, only symmetrical distributions are explored where, $\alpha = \beta = 0, 1, 2, 4, 8, 16, 32$ in the interval 0.001 to 0.01 cm. Fig. 2 shows a plot of the cumulative probability distributions used in this study. Pore radii are distributed randomly within the regular two-dimensional network. For each distribution considered here, we keep the global hierarchy (i.e., order for the field) identical. Thus, all differences seen in the results presented below are due entirely to the combination of pore-size distribution, pore shape (facilitation), network connectivity (coordination of 4 or 8), and angle in the gravity field (horizontal or vertical). Evaluation of the pore networks, assuming thermodynamic equilibrium with $r_1 = r_p$ and $\theta = 0$ (i.e., all pores are equally accessible for filling with no facilitation, trapping, or hysteresis), yields fluid retention curves relating pressure potential to network saturation for the wetting fluid as shown in Fig. 3.

A simulation is started by making all pores in the top row of the network available for filling (top 256 pores). These pores are searched to find the pore with the lowest filling potential and this pore is filled. The list of pores available to be filled is then adjusted to remove those pores that have become entrapped and include those adjacent to the newly filled pore. Filling potentials are then recalculated to include any change due to facilitation and the list is again searched for the pore with the lowest filling potential, and so on. These simulations model the imbibition of water through the combined action of capillary and gravity forces into the top of a vertical, air filled porous media ($\gamma = 0$ degrees). Air is allowed to move freely out the sides and bottom of the network. For comparison purposes, the model is also run without gravity ($\gamma = 90$

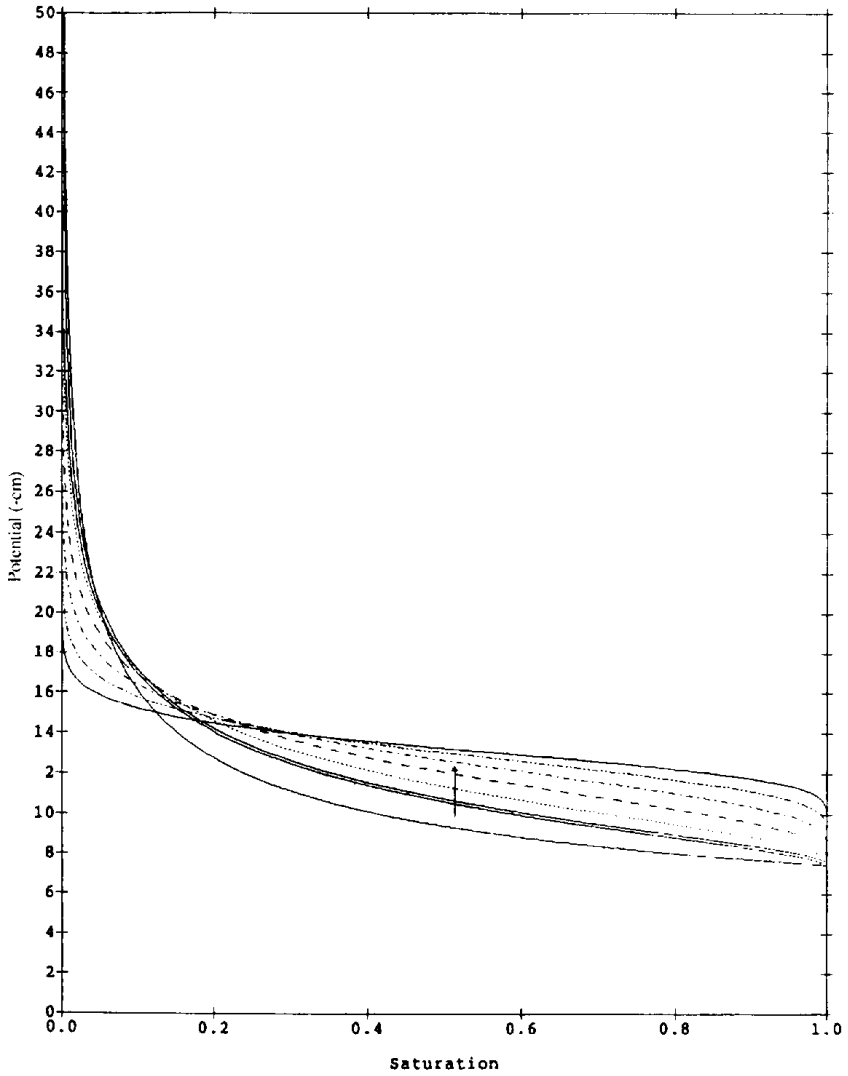

Fig. 3. Evaluation of the pore networks with pore-size distributions shown in Fig. 2, and assuming thermodynamic equilibrium with $r_t = r_p$ and $\theta = 0$ (i.e., all pores are equally accessible for filling with no facilitation, trapping, or hysteresis), yields an equilibrium fluid retention curve relating pressure potential to network saturation for the wetting fluid. Increasing $\alpha = \beta$ is denoted by the arrow.

degrees) to simulate horizontal imbibition and without facilitation so that $r_t = r_p$. The combination of no facilitation and no gravity collapses the MIP model to that of IP.

4. Results

The sequential development of the wetted structure as water is imbibed into the horizontal network without facilitation in coordination of 4 is shown in Fig. 4. The wetted structure at network breakthrough for the same situation in coordination of 8 with crossing necks is shown in Fig. 5. For these and all other simulations presented here,

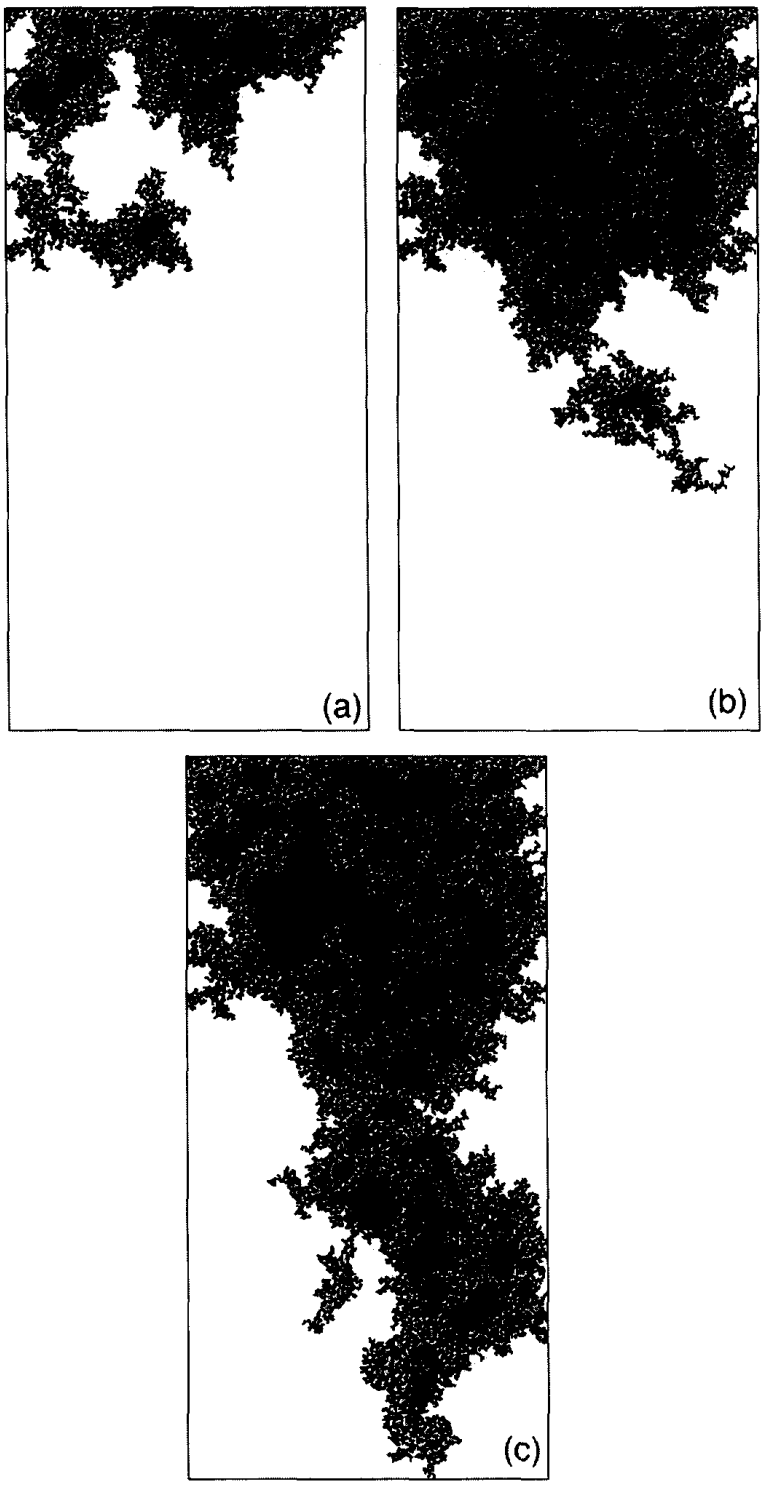

Fig. 4. Horizontal imbibition, no facilitation in coordination 4. Wetted structure is shown at three positions as water is imbibed into the network under capillary forces. Black denotes water, gray entrapped air, and white unentrapped, mobile air.

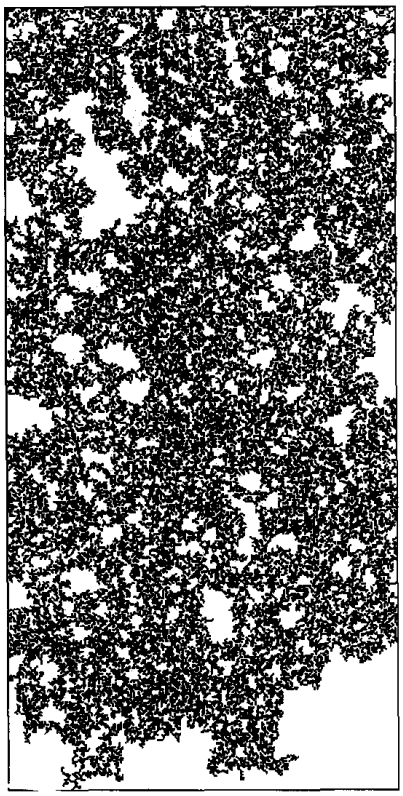

Fig. 5. Horizontal imbibition, no facilitation in coordination 8. Wetted structure at network breakthrough. Black denotes water, gray entrapped air and white unentrapped, mobile air.

black denotes the water phase, white the air phase that is free to move out of the network, and gray the entrapped air phase. Wetted structure growth is seen to occur in small "capillary fingers" that have no particular orientation and most often grow back on themselves. The wetted structure is found to be very complicated at all scales down to the pore-scale and has been shown to be fractal (Wilkinson and Willemsen, 1983). In addition, the wetted structure that evolves is independent of the pore-size distribution ($\alpha = \beta = 0$, 1, 2, 4, 8, 16, 32 all give identical results) and a function of only the pore hierarchy or structural order within the random field. Important differences between a coordination of 4 and 8 in the wetted structures and magnitude of air entrapment can be seen in Figs. 4 and 5. At the point when water first reaches the end of the network, only water exists as a continuum in coordination of 4. With a coordination of 8, a bi-continua of air and water exists with very little phase entrapment. This result exemplifies the distinction between two- and three-dimensional networks. All these results are identical to those found for IP by others (e.g., Wilkinson and Willemsen, 1983) and provide a point of comparison for the MIP model incorporating gravity and facilitation.

For vertical downward infiltration without facilitation, gravity influences the growth of small capillary fingers yielding an overall downward preference (see Fig. 6). A single vertically oriented macroscopic finger results which is composed of a sequence of larger clusters where small capillary fingers have grown back on themselves strung together by

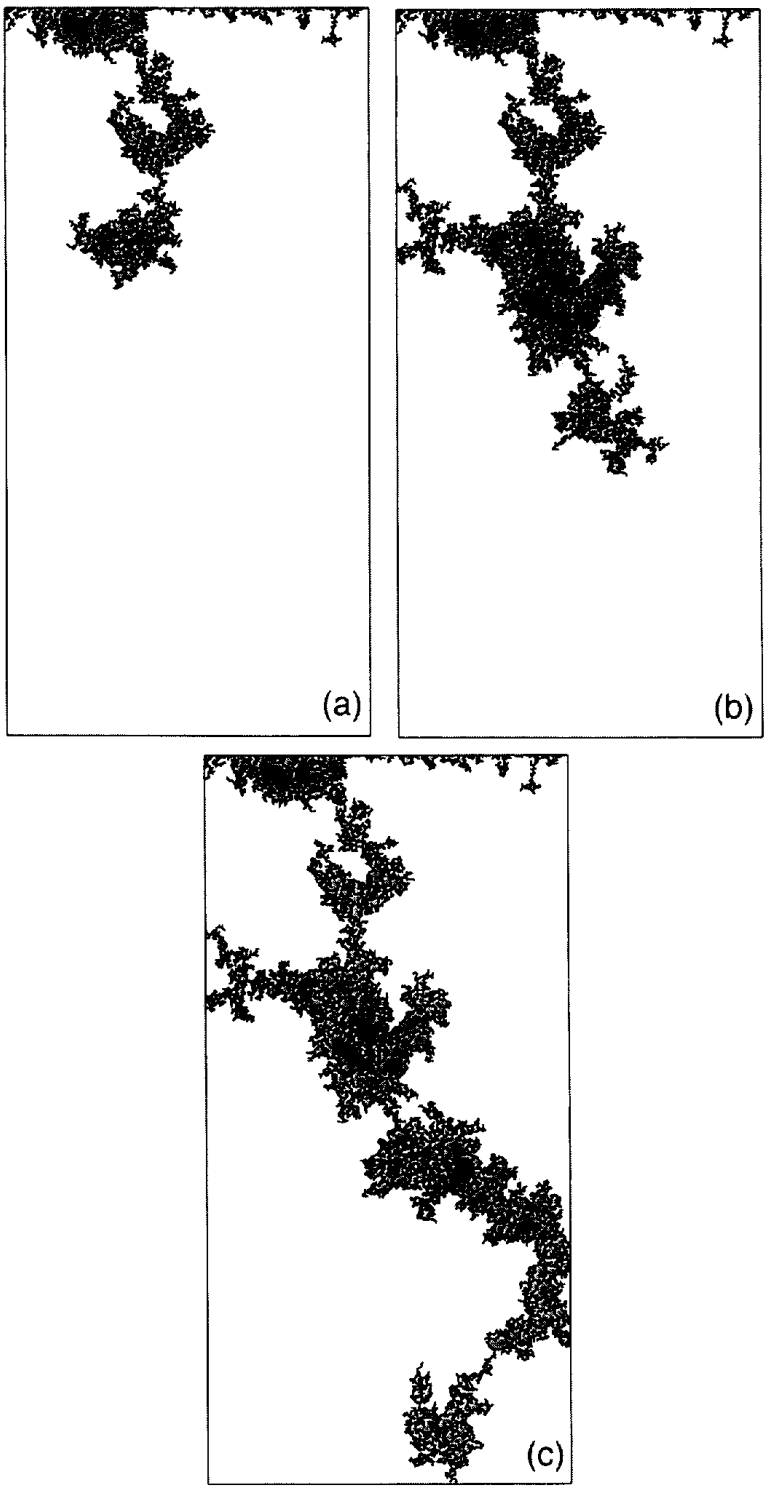

Fig. 6. Vertical downward infiltration, no facilitation in coordination 4. Wetted structure is shown at three positions as water is imbibed into the network under capillary and gravity forces. Black denotes water, gray entrapped air, and white unentrapped, mobile air.

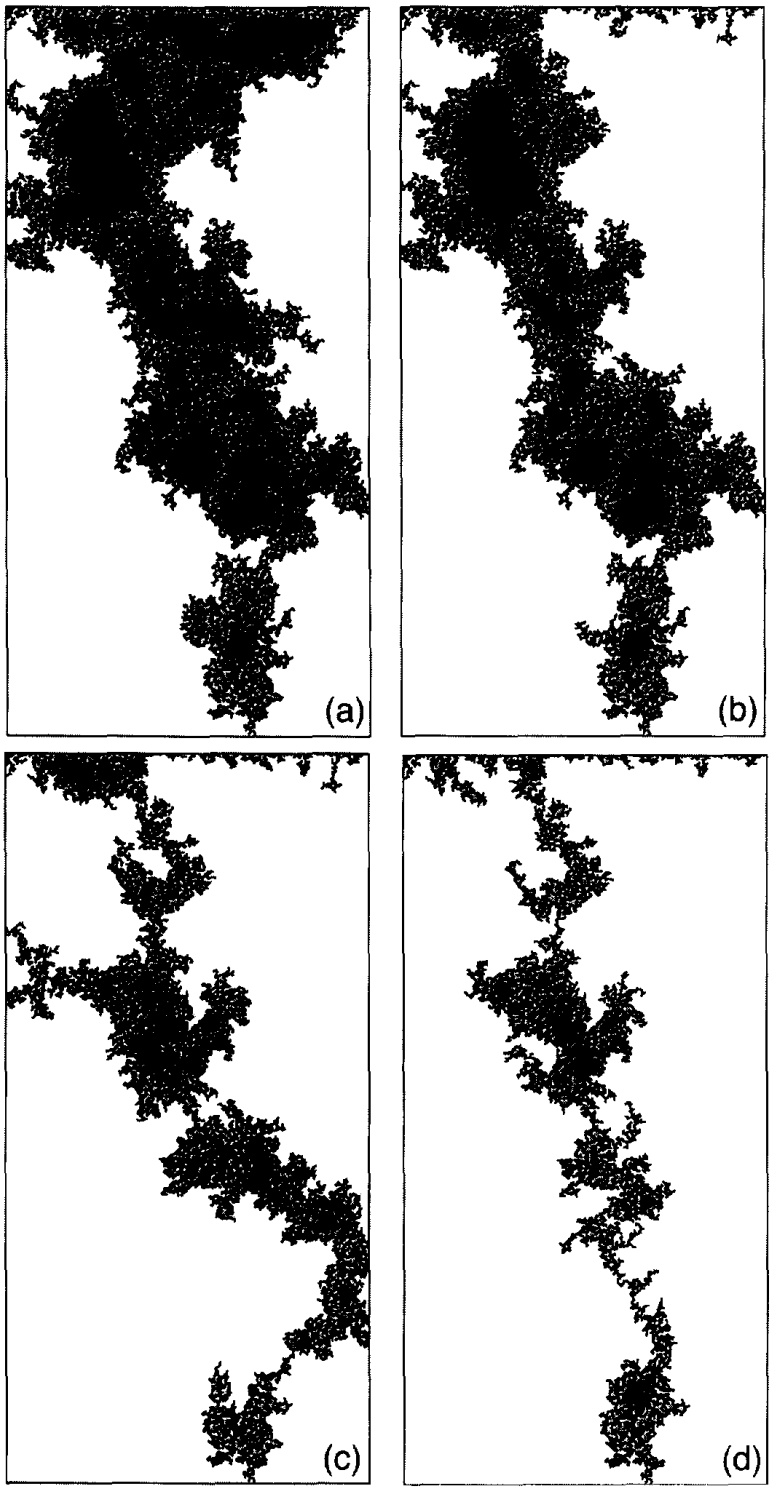

Fig. 7. Vertical downward infiltration, no facilitation in coordination 4. Wetted structure at network breakthrough for $\beta = \alpha$ of 0 (a), 2 (b), 8 (c), and 32 (d). Black denotes water, gray entrapped air, and white unentrapped, mobile air.

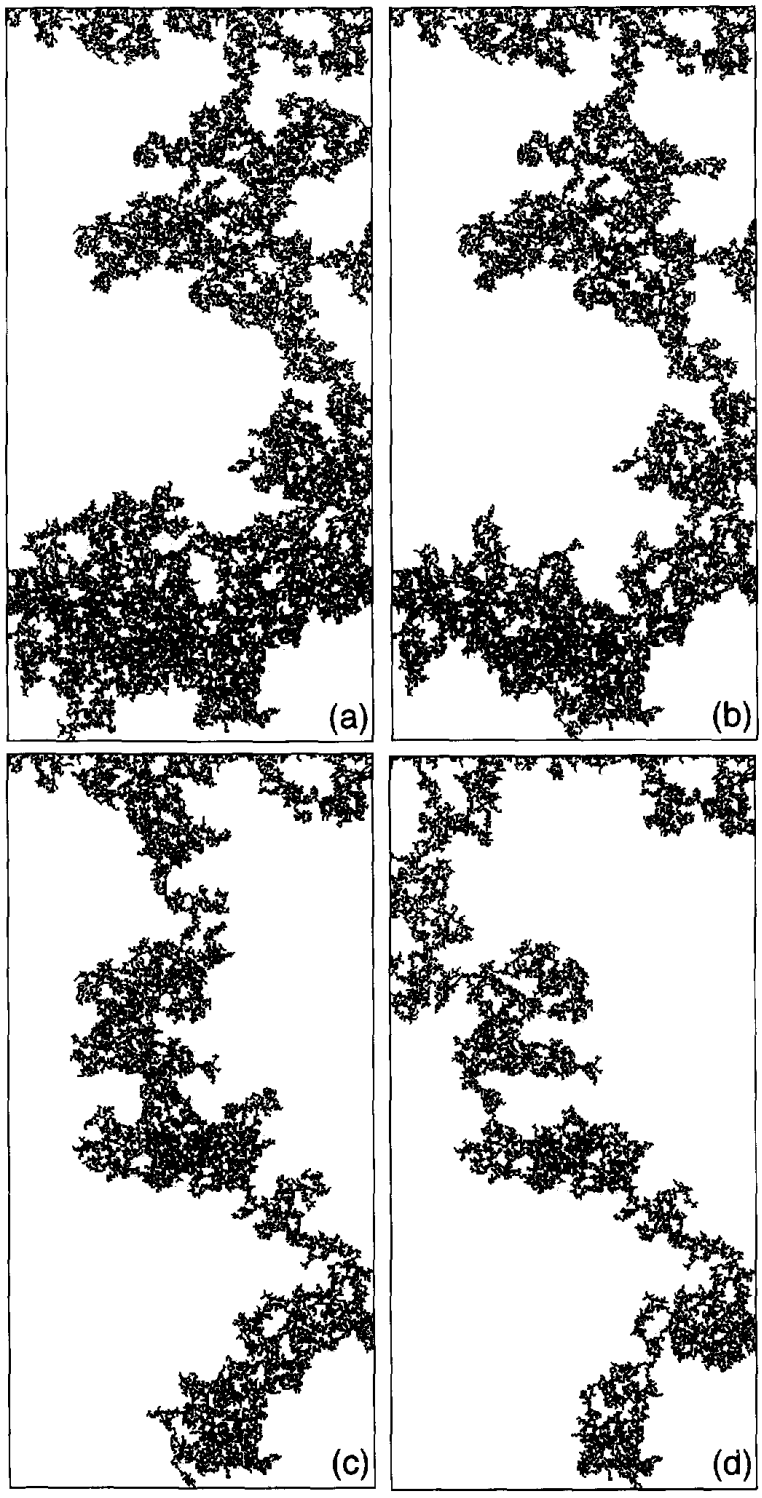

Fig. 8. Vertical downward infiltration, no facilitation in coordination 8. Wetted structure at network breakthrough for $\beta = \alpha$ of 0 (a), 2 (b), 8 (c), and 32 (d). Black denotes water, gray entrapped air, and white unentrapped, mobile air.

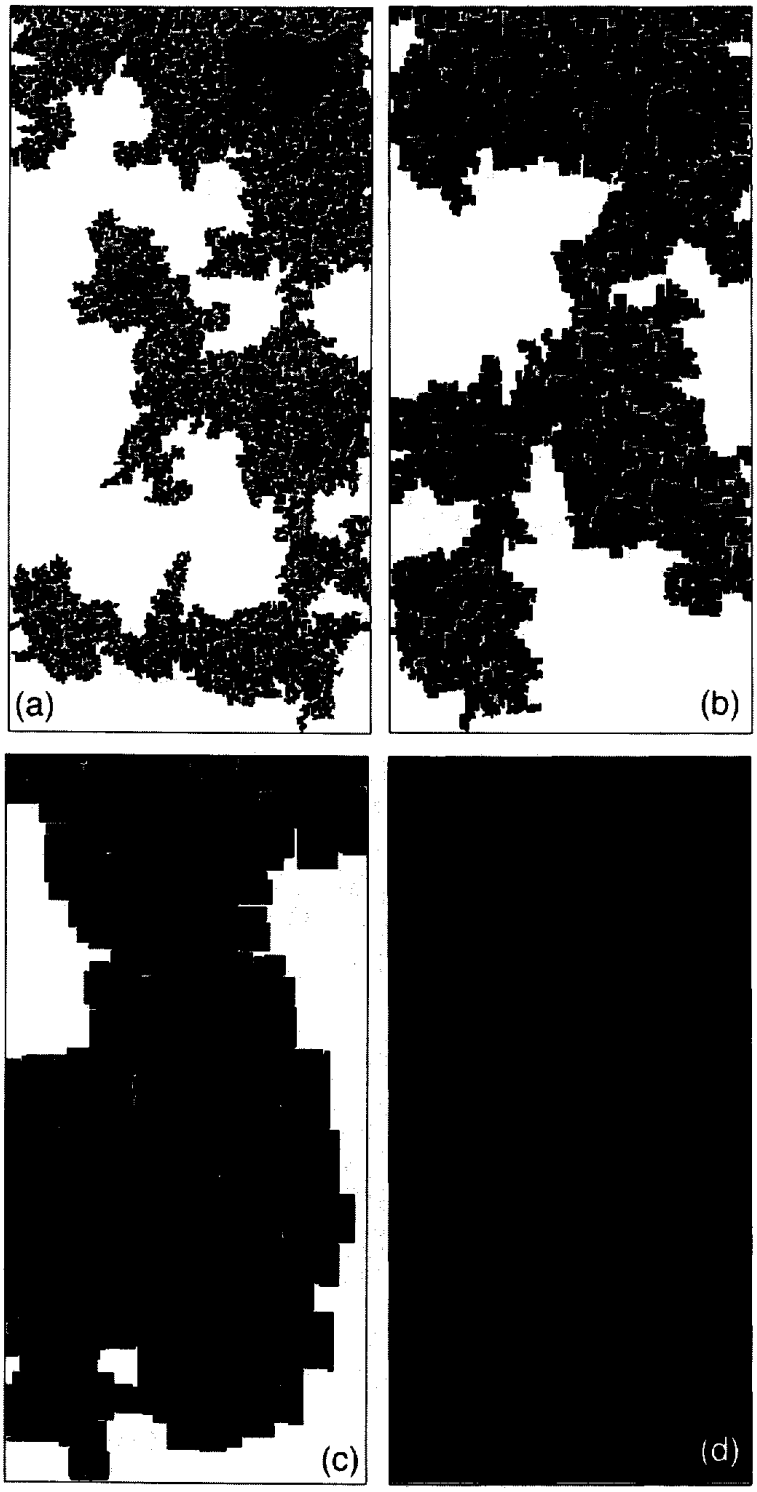

Fig. 9. Horizontal imbibition, square pores. Wetted structure at network breakthrough for $\beta = \alpha$ of 0 (a), 2 (b), 8 (c), and 32 (d). Black denotes water, gray entrapped air, and white unentrapped, mobile air. Note that in (d), the network was entirely filled with water (black) at breakthrough.

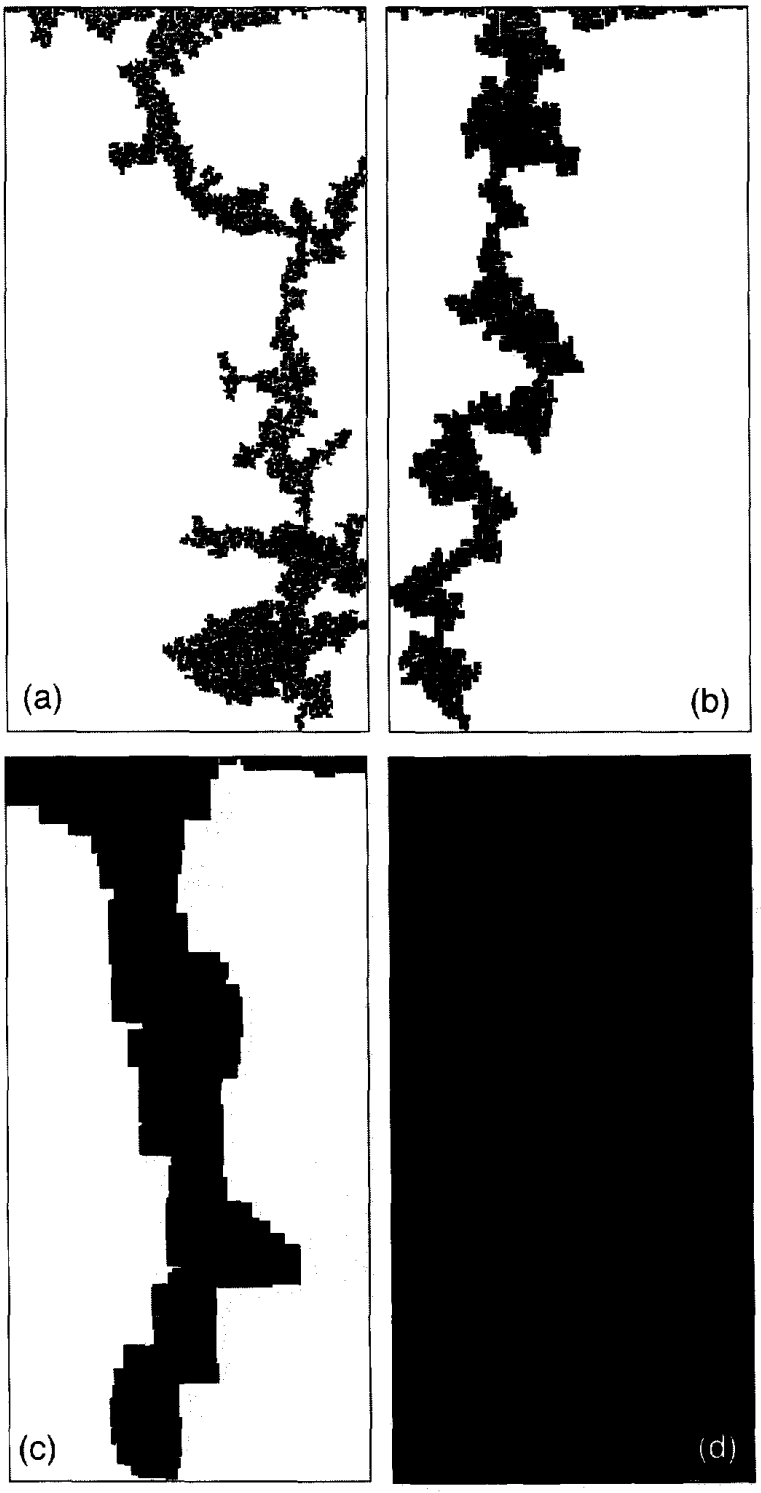

Fig. 10. Vertical downward infiltration, square pores. Wetted structure at network breakthrough for $\beta = \alpha$ of 0 (a), 2 (b), 8 (c), and 32 (d). Black denotes water, gray entrapped air, and white unentrapped, mobile air. Note that in (d), the network was entirely filled with water (black) at breakthrough.

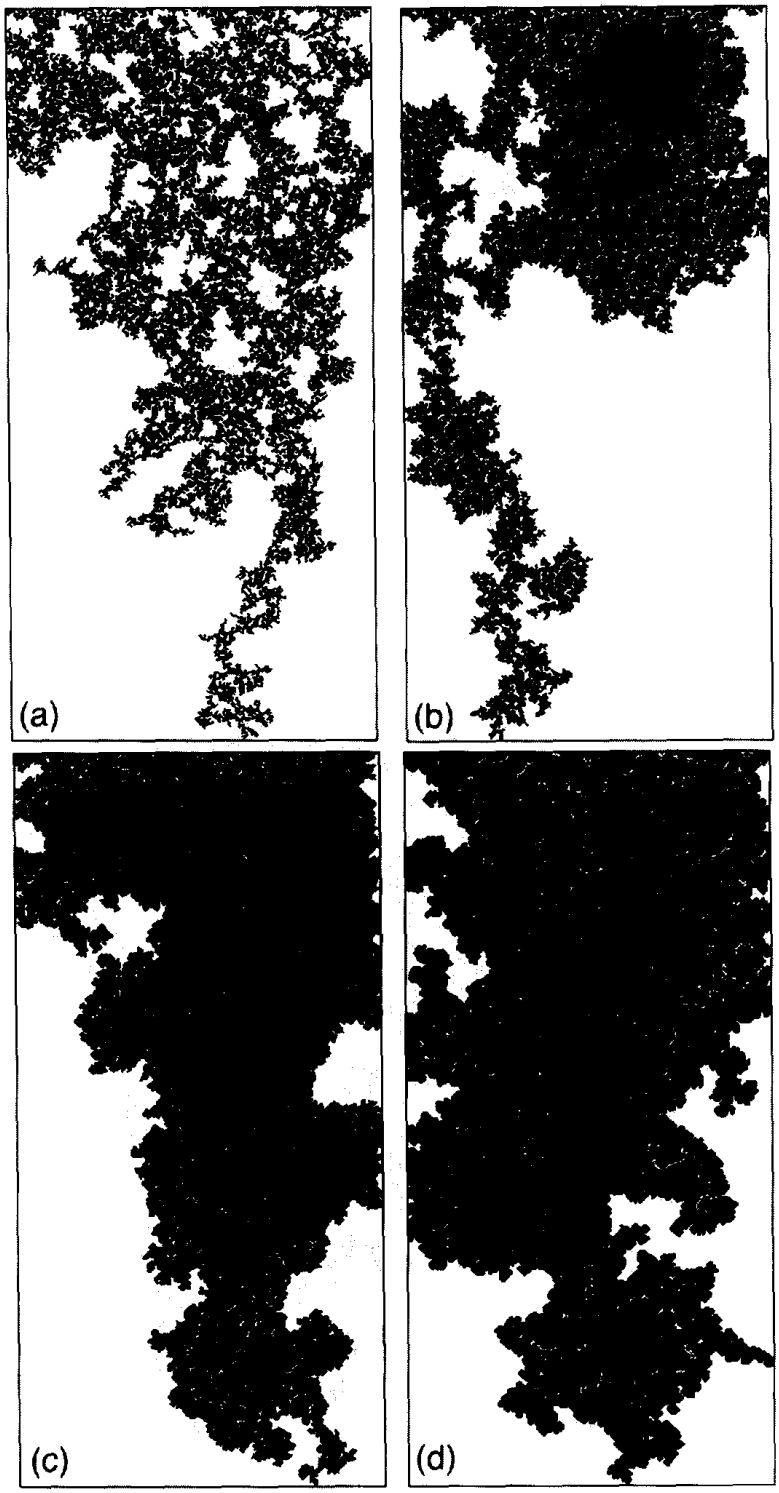

Fig. 11. Horizontal imbibition, octagon pores. Wetted structure at network breakthrough for $\beta = \alpha$ of 0 (a), 2 (b), 8 (c), and 32 (d). Black denotes water, gray entrapped air, and white unentrapped, mobile air.

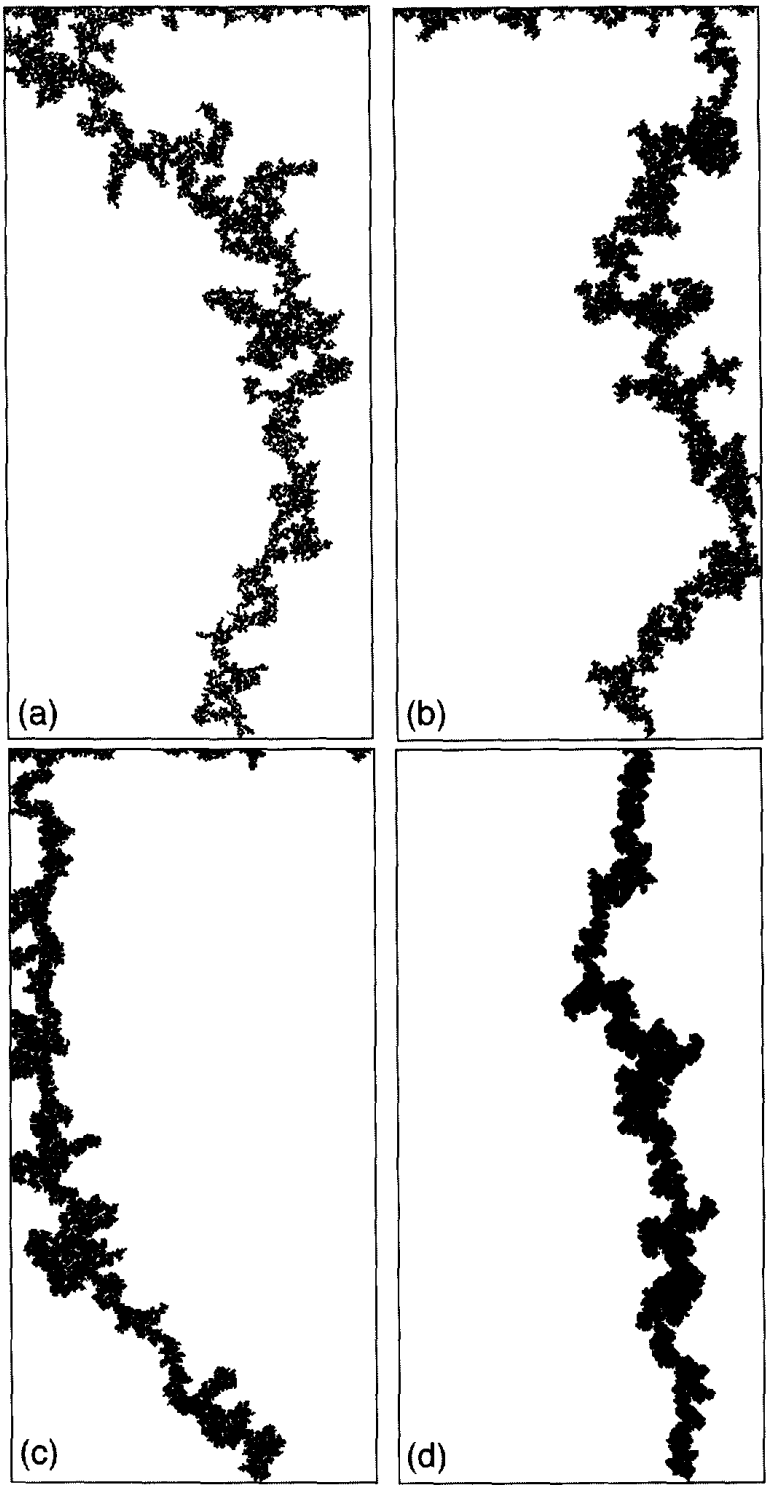

Fig. 12. Vertical downward infiltration, octagon pores. Wetted structure at network breakthrough for $\beta = \alpha$ of 0 (a), 2 (b), 8 (c), and 32 (d). Black denotes water, gray entrapped air, and white unentrapped, mobile air.

narrow zones at the scale of a single capillary finger often only a single pore wide. Figs. 7 and 8 show the finger structures at network breakthrough for $\alpha = \beta = 0, 2, 8, 32$ for a coordination of 4 and 8, respectively. Macroscopic finger width is observed to be a function of the pore-size distribution; as the distribution narrows, capillary fingering is more influenced by gravity and macroscopic finger width decreases. While such a pore-scale fingering pattern may be qualitatively similar to gravity nonwetting fluid fingering, the highly complicated geometry of the finger edges does not compare well with the much smoother edges observed in gravity wetting fluid fingering (Glass et al., 1989b).

Consideration of pore geometry demonstrates the effects of facilitation. For both the idealized square and octagonal two-dimensional pores, macroscopic fronts are seen to form both during horizontal imbibition (Fig. 9 and Fig. 11) and vertical downward infiltration with gravity (Fig. 10 and Fig. 12). These macroscopic fronts create more compact wetted structures with less entrapped air phase. Wetted region structure is also affected by pore-size distributions. For squares, an increase in $\alpha = \beta$ increases the macroscopic smoothing effect such that at $\alpha = \beta = 32$ the front becomes flat across the network with or without gravity (Fig. 9d and Fig. 10d). This occurs because $[r_{max} - r_{min}] < 0.5 r_{max}$ and all the pores in one row will fill due to facilitation before any pores in the next row are filled ($\alpha = \beta = 32$ is above this limit, see Fig. 3). Octagons behave similarly to squares but with less smoothing of the interface, as is expected from the additional connections and calculations for r_1 (Table 1). In contrast to behavior observed for square pores, at $\alpha = \beta = 32$, the front is far from flat for the octagon pore geometry in Fig. 11d and Fig. 12d. Additional simulations were performed with the octagon pore network for narrower distributions yielding a similar domination of smoothing for $\alpha = \beta \sim 512$, with or without gravity. The facilitation dominated structure has an octagon-like pattern, emphasizing that for both the squares and octagons, the connectivity in combination with the regular grid chosen for our simulations clearly influences the substructure and creates blocky (flat) or octagon-like subunit artifacts.

Finger width was measured on the vertical simulations. The finger edges were taken to be the first and last pores encountered that were filled with water in a horizontal row. The difference between these two edges was used as the local finger width. Neglecting the top 10% and the bottom 10% of the field where boundary effects were significant,

Table 2
Calculated finger widths (cm)

$\alpha = \beta$	Coordination four squares	Standard deviation	Coordination four no facilitation	Standard deviation	Coordination eight octagons	Standard deviation	Coordination eight no facilitation	Standard deviation
0	1.1789	0.4189	0.6038	0.4497	1.3896	0.7268	0.505	0.3514
1	1.0247	0.41057	0.3666	0.1834	1.3051	0.7191	0.45	0.2951
2	1.0236	0.4114	0.43	0.2106	1.2245	0.7626	0.4015	0.2276
4	0.8048	0.3632	0.4861	0.1912	1.1838	0.7081	0.4323	0.2571
8	0.7272	0.3881	0.6426	0.1697	0.7048	0.3458	0.3064	0.1374
16	0.6554	0.3732	1.7655	0.1641	0.6291	0.3306	0.3018	0.1652
32	0.4748	0.2836	–	–	0.7255	0.42	0.3007	0.1313

the average and standard deviation of the local finger widths were calculated. Table 2 shows the behavior of the finger width and standard deviation as a function of pore-size distribution ($\alpha = \beta$).

5. Discussion

The MIP model yields much different imbibition front structures than IP for wetting fluids (in this case, water) advancing into networks initially filled with a non-wetting fluid (in this case, air). For MIP on random networks, capillary fingering, capillary facilitation, and gravity fingering compete to determine the wetted network structure as a function of pore-size distribution. Over different portions of the parameter ranges, each process can dominate over the others. Where pore-size distribution is sufficiently wide, variability in capillary pressure potential from pore to pore dominates structural evolution, and near-pore-scale, non-directional capillary fingering occurs (see Fig. 9a and Fig. 11a). Where the pore-size distribution is sufficiently narrow, capillary facilitation dominates, the saturation front is smooth and water moves across the network from the supply surface in one macroscopic front (see Fig. 9d and Fig. 10d). At intermediate pore-size distributions, gravity dominates and a single gravity finger moves in close alignment with the gravitational vector (see Figs. 10c and 12d).

These results suggest capillary forces to stabilize downward infiltration events either in very narrow or very wide pore-size distribution media. While this stabilization is intuitive for wide pore-size distributions, gravity fingering has generally been considered to dominate as the pore-size distribution narrows. For very narrow distributions, it is probable that to overwhelm capillary facilitation smoothing, perturbation wavelength must be above a lower limit. This, of course, is analogous to the stabilization provided by an effective surface tension incorporated in the linear stability analysis of Chouke et al. (1959). It is also possible that the amplitude of the perturbation must also be above a lower limit for a gravity finger to form, especially where facilitation fully dominates displacement (e.g., see Fig. 10d for the square pores). In this case, the wavelength of this large amplitude perturbation will likely determine finger width as has been seen in experiments conducted in fractures (Nicholl et al., 1994).

For MIP to capture the downward moving saturated finger tip with drainage behind, incorporation of simultaneous wetting and drainage within a single simulation is required. A separate size distribution for the smaller necks must be incorporated along with the redefinition of the gravitational potential (Eq. 2) to apply only within connected fluid regions. It is important to note that this analytic complication is not required for MIP to generate gravity fingers and the water swept structure. The critical aspect of finger growth is the incorporation of the hanging column effect in the definition of the gravitational potential to yield a total potential within the finger that is hydrostatic, with the pressure potential decreasing upward from the back of the finger tip.

Qualitatively, macroscopic finger structure seen in experiments in porous media (Glass et al., 1989c) is very similar to that demonstrated by the MIP in Fig. 10c for squares ($\alpha = \beta = 8$) and Fig. 12d for octagons ($\alpha = \beta = 32$). While pore-size distributions were chosen to span a range that was representative of previously used experimen-

tal sands, the fact that ideal two-dimensional pore geometries were assumed (r_2 infinite) makes quantitative comparison of modeled and experimentally determined finger widths difficult. For a three-dimensional pore, additional contribution to the total potential from capillary forces may be as great as a factor of two. Facilitation may also act on both r_1 and r_2, depending on the pore geometry, so that its effect may be more important than in the two-dimensional pores. Alternatively, facilitation may act only on one of the two radii of curvature and, thus, its effect diminished as the other radius becomes of the same order or smaller. Regardless of these limitations, quantitative agreement with measured finger widths in experimental sands is quite reasonable. The 14–20 mesh sand used in the experiments of Glass et al. (1989b) yielded a finger width of approximately 1 cm in the low flow limit. Comparison to Table 2 shows the finger width for most pore-size distributions to be within a factor of two and many within one standard deviation of the physical experimental results. At present, experiments considering the effects of pore-size distribution on finger formation and resulting finger width, have not been conducted. Based on our model results, a series of experiments and numerical simulations should be conducted to test the hypothesized system behavior as a function of pore-size distribution. For these comparisons, MIP should be implemented for a three-dimensional network with capillary facilitation functions developed for three-dimensional pores.

It must be emphasized that MIP does not include the influence of viscous forces or time. The MIP analysis is restricted to situations where the flow rates are low but at the same time high enough that fluxes due to film flow are negligible. Since viscous forces stabilize gravity fingering, exploration of the quasi-static limit with approaches such as MIP allows us to investigate the importance of a variety of factors that may also stabilize fluid displacements where current theory suggests gravity fingering to occur. In addition, under many natural gradient conditions within the vadose zone, flows are slow and viscous forces are small relative to capillary and gravitational forces. From this perspective, MIP should yield behavior representative of many natural field situations.

Finally, two differences between MIP and IP of a more theoretical nature are worth mentioning. The first is that when gravity fingers form, MIP supports the existence of a directional bi-continua in a truly two-dimensional network. If the width of the network is larger than the finger width, then both air and water pathways exist vertically, yielding a vertical bi-continua. As a consequence, neither phase is laterally continuous across the system. Secondly, a macroscopic length scale for IP does not exist, whereas for MIP when gravity fingers form, a length scale on the order of the finger width can be defined. These results are significant for understanding two-phase flow in single fractures where a two-dimensional pore network is a reality (Glass, 1993).

6. Conclusion

The Haines jump pore-filling mechanism responsible for pore-scale finger tip growth is mimicked by the invasion percolation process. The inclusion of gravity into invasion percolation models yields gravity fingers. Adjacent-neck–pore-filling facilitation, which incorporates a pore-scale geometric interfacial capillary smoothing function into inva-

sion percolation models, causes the formation of macroscopic fronts, and in combination with gravity, macroscopic fingers. These qualitative results compare favorably with those of physical experiments for wetting fluid invasion of a porous media where macroscopic fronts and gravity fingers form.

A large number of physical situations and system parameters can be evaluated with the MIP model. These include: the influence of contact angle, the shape of the pore-size distribution, heterogeneities, initial fluid content, and other fluid/fluid systems such as NAPL/air and NAPL/water. The major constraints of this model are simply that viscous forces be small with respect to capillary and gravity forces, and that non-pore-filling mechanisms such as film flow are negligible. Thus MIP will not capture dynamic aspects of fingering at high flow rates as studied by Glass et al. (1989b) and others. An additional limitation in the current implementation is the overly simplistic representation of the pore network as a regular grid composed of two-dimensional pores of ideal geometry connected by necks of much smaller size. These limitations, however, can be relaxed as more realistic networks and facilitation rules are developed to better represent natural three-dimensional systems.

Acknowledgements

The substance of this paper was presented orally at the December 1989 American Geophysical Union meeting (Glass and Yarrington, 1989) and the American Society of Agricultural Engineering National Symposium on Preferential Flow in December 1991. The authors thank M.J. Nicholl, S. Conrad, and P.B. Davies of Sandia National Laboratories for careful review of the manuscript.

References

Adler, P.M., Jacquin, C.G. and Thovert, J.-F., 1992. The formation factor of reconstructed porous media. Water Resour. Res., 28: 1571–1576.

Chouke, R.L., Van Meurs, P. and Van der Poel, C., 1959. The instability of slow immiscible, viscous liquid–liquid displacements in porous media. Trans. Am. Inst. Min. Eng., 216: T.P.8073.

Glass, R.J., 1993. Modeling gravity driven fingering in rough-walled fractures using modified percolation theory. Proc. 4th Int. Conf. on High Level Radiation Waste Management, American Nuclear Society, April 26–30, Las Vegas, NV, pp. 2042–2053.

Glass, R.J. and Nicholl, M.J., 1996. Physics of gravity fingering of immiscible fluids within porous media: An overview of current understanding and complicating factors. Geoderma, 70: 133–163, this issue.

Glass, R.J. and Yarrington, L., 1989. Analysis of wetting front instability using modified invasion percolation theory. EOS, 70: 1117.

Glass, R.J., Parlange, J.-Y. and Steenhuis, T.S., 1989a. Wetting front instability I: Theoretical discussion and dimensional analysis. Water Resour. Res., 25: 1187–1194.

Glass, R.J., Steenhuis, T.S. and Parlange, J.-Y., 1989b. Wetting front instability II: Experimental determination of relationships between system parameters and two-dimensional unstable flow field behavior in initially dry porous media. Water Resour. Res., 25: 1195–1207.

Glass, R.J., Steenhuis, T.S. and Parlange, J.-Y., 1989c. Mechanism for finger persistence in homogeneous unsaturated porous media: Theory and verification. Soil Sci. 148: 60–70.

Harr, M.E., 1987. Reliability-Based Design in Civil Engineering. McGraw-Hill, New York, p. 93.

Lenormand, R. and Zarcone, C., 1984. Growth of clusters during imbibition in a network of capillaries. In: F. Family and D.P. Landau (Editors), Kinetics of Aggregation and Gelation. Elsevier, Amsterdam, pp. 177–181.

Lenormand, R. and Zarcone, C., 1985. Invasion percolation in an Etched Network: Measurement of a fractal dimension. Phys. Rev. Lett., 54: 2226–2229.

Nicholl, M.J., Glass, R.J. and Wheatcraft, S.W., 1994. Gravity-driven infiltration instability in initially dry non-horizontal fractures. Water Resour. Res., 30(9): 2533–2546.

Saffman, P.G. and Taylor, G.I., 1958. The penetration of a fluid into a porous medium or Hele–Shaw cell containing a more viscous liquid. Proc. R. Soc. Lond., A245: 312–331.

Wilkinson, D., 1984. Percolation model of immiscible displacement in the presence of buoyancy forces. Phys. Rev. A., 30: 520–531.

Wilkinson, D. and Willemsen, J.F., 1983. Invasion percolation: A new form of percolation theory. J. Phys. A (Math. Gen.), 16: 3365–3376.